

# JOURNAL OF THE AMERICAN CHEMICAL SOCIETY

## A Gas-Phase Study of $\text{FeS}_n^+$ ( $n = 1-6$ )

T. J. MacMahon, T. C. Jackson,<sup>†</sup> and B. S. Freiser\*

Contribution from the Department of Chemistry, Purdue University,  
West Lafayette, Indiana 47907. Received January 27, 1988

**Abstract:** Photodissociation, collision-induced dissociation (CID), ion-molecule reactions, and kinetics experiments were used to study the series  $\text{FeS}_n^+$  ( $n = 1-6$ ) generated from sequential reactions of  $\text{Fe}^+$  with ethylene sulfide in the gas phase.  $\text{FeS}_n^+$  ( $n = 0-5$ ) were observed to react with ethylene sulfide by linear pseudo-first-order kinetics for over 2.5 half-lives, indicating that the ions were formed predominantly in their ground states and in one isomeric form for each ion studied.  $\text{FeS}_6^+$ , however, was not observed to react with ethylene sulfide.  $D^\circ(\text{Fe}^+-\text{C}_2\text{H}_2) = 32 \pm 6$  kcal/mol was determined by ion-molecule reactions. In addition, photodissociation thresholds gave the following bond energies directly:  $D^\circ(\text{Fe}^+-\text{S}) = 61 \pm 6$  kcal/mol,  $D^\circ(\text{Fe}^+-\text{S}_2) = 48 \pm 5$  kcal/mol,  $D^\circ(\text{FeS}^+-\text{S}_2) = 49 \pm 5$  kcal/mol,  $D^\circ(\text{FeS}_2^+-\text{S}_2) = 49 \pm 5$  kcal/mol, and  $D^\circ(\text{FeS}_3^+-\text{S}_2) = 43 \pm 5$  kcal/mol. Photodissociation and ion-molecule reactions were used to assign  $D^\circ(\text{FeS}_4^+-\text{S}_2) = 38 \pm 5$  kcal/mol. These bond energies yield a variety of other thermochemical data. The implications of these results to ion structure are discussed.

Polysulfide chelates of transition metals have been of recent interest to inorganic chemists because of their wide variety of reactivities and structures. These complexes include sulfurs bound to metal centers individually, as in  $\text{VS}_4^{3-}$  and  $\text{ReS}_4^-$ ,<sup>1</sup> and in rings, as in  $(\eta^5\text{-C}_5\text{Me}_5)_2\text{ThS}_5^2$  and  $\text{MoS}_9^{2-}$ .<sup>3</sup> In addition, although sulfides are less reactive catalysts than their corresponding oxides or bare metals, they show less susceptibility to poisoning and in some cases may even be more selective.<sup>4</sup> In order to understand these results, it may be useful to characterize the intrinsic properties of iron sulfides, which is one of the aims of this study. Another important aspect of this work is to investigate the synergistic effects of one or more ligands on the bond energy of another. The understanding gained in these types of studies is important in bridging the gap between gas-phase and solution-phase chemistry. The series  $\text{FeS}^+$  through  $\text{FeS}_6^+$  provides a unique system to probe these questions.

### Experimental Section

The theory, instrumentation, and methodology of Fourier transform mass spectrometry (FTMS) have been discussed elsewhere.<sup>5</sup> The two Fourier transform mass spectrometers used in this study were a prototype FTMS-1000 and an FTMS-2000, both from Nicolet and each equipped with a Quanta-Ray Nd:YAG laser.  $\text{Fe}^+$  was generated by focusing the fundamental or frequency doubled line of the laser onto a high purity block of iron metal as has been discussed elsewhere.<sup>6</sup> The FTMS-1000

has a 5.2-cm cubic cell, which is situated between the poles of a Varian 15-in. electromagnet maintained at  $\sim 0.9$  T. The two transmitter plates were replaced with 80% transmittance stainless steel screens. These screens allowed the ions in the cell to be irradiated by light from a 2.5-kW Hg-Xe arc lamp used in conjunction with a 0.25-m Schoeffel monochromator set at 10-nm resolution.

The FTMS-2000 is equipped with a differentially pumped dual analysis cell with two 4.8-cm cubic cells that share a common side known as the conductance limit. The conductance limit contains a 1-mm radius hole for use in transferring ions from one cell to the other; however, in this study only one side of the dual analysis cell was used. The entire cell is situated in the bore of a 3-T superconducting magnet.

With both instruments, chemicals were either leaked into the cell from a Varian leak valve in order to maintain a constant background pressure

- (1) Do, Y.; Simhon, E. D.; Holm, R. H. *Inorg. Chem.* **1985**, *24*, 4635.
- (2) Wroblewski, D. A.; Cromer, D. T.; Ortiz, J. V.; Rauchfuss, T. B.; Ryan, R. R.; Sattelberger, A. P. *J. Am. Chem. Soc.* **1986**, *108*, 174.
- (3) (a) Draganjac, M.; Simhon, E.; Chan, L. T.; Kanatzidis, M.; Baenziger, N. C.; Coucouvanis, D. *Inorg. Chem.* **1982**, *21*, 3321. (b) Coucouvanis, D.; Hadjikyriacou, A.; Draganjac, M.; Kanatzidis, M. G.; Illeperuma, O. *Polyhedron* **1986**, *5*, 349.
- (4) (a) Mitchell, P. C. H.; Ckemball, I. N., Eds.; *Catalysis; The Chemical Society: London, 1981; Vol. 4.* (b) Bhadure, M.; Mitchell, P. C. H. *J. Catal.* **1982**, *77*, 132.
- (5) (a) Comisarow, M. B. *Adv. Mass Spectrom.* **1980**, *8*, 1698. (b) Gross, M. L.; Rempel, D. L. *Science* **1984**, *226*, 261. (c) Marshall, A. G. *Acc. Chem. Res.* **1985**, *18*, 316. (d) Freiser, B. S. *Talanta* **1985**, *32*, 697.
- (6) Cody, R. B.; Burnier, R. C.; Reents, W. D., Jr.; Carlin, T. J.; McCrery, D. A.; Lengel, R. K.; Freiser, B. S. *Int. J. Mass Spectrom. Ion Phys.* **1980**, *33*, 37.

<sup>†</sup>Current address: Eastman Kodak Co., Rochester, NY 14650.

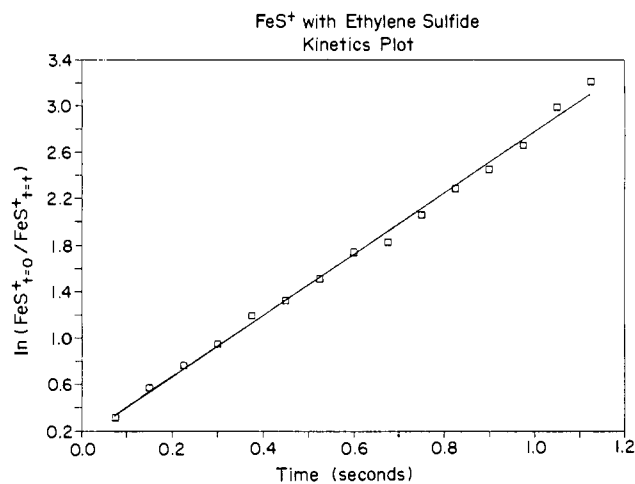


Figure 1. Kinetics plot for  $\text{FeS}^+$  with ethylene sulfide.

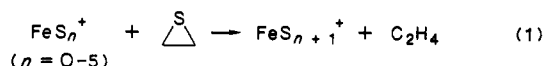
or pulsed into the cell using a General Valve Corp. Series 9 pulsed solenoid valve.<sup>7</sup> The pulse profile on the FTMS-1000 was such that the pressure peaked about 200 ms after firing the valve and was pumped away in about 500 ms. The FTMS-2000 pulsed gas profile had a rise time of about 400 ms after which the gas was pumped away in about 600 ms. All chemicals were used as supplied except for liquids which were subjected to multiple freeze-pump-thaw cycles to remove any noncondensable gases. Pressures were measured with an uncalibrated Bayard-Alpert ionization gauge.

The two instruments were used interchangeably, except that all of the photodissociation experiments were carried out using the prototype FTMS-1000 equipped with the arc lamp. To ensure that the ions studied were thermal, they were allowed to collide with argon at a background pressure of  $5 \times 10^{-6}$  Torr for 0.5 to 2 s depending on the particular ion, permitting the ions to undergo approximately 40 to 160 collisions with argon.<sup>8</sup> Following this period, all ions were eliminated from the cell by ejection pulses, except for a selected ion. This ion was then probed by either photodissociation, collision-induced dissociation (CID), or further reaction.

The photodissociation spectra were obtained by plotting  $\ln(1 + \text{intensity of the ion photoproducts/intensity of the parent ion})$  versus wavelength.<sup>9</sup> The estimated uncertainty of the photodissociation peak intensities is  $\pm 40\%$  and peak locations is  $\pm 10$  nm. Thresholds were obtained using cutoff filters characterized on a UV-vis spectrometer, and the filter cutoffs were assigned at approximately 1% transmittance. Absolute cross sections were determined by referencing the photodissociation of  $\text{FeS}^+$  monitored at 320 nm ( $\sigma_{320} = 0.3 \text{ \AA}^2$ )<sup>15</sup> to the photodissociation of the ion of interest at its  $\lambda_{\text{max}}$ . The cross sections determined in this manner have an estimated uncertainty of  $\pm 50\%$  due to instrumental variables.

CID was performed as previously described<sup>10</sup> and argon was used as the collision gas at a pressure of  $\sim 1 \times 10^{-5}$  Torr. The collision energy of the ions can be varied typically between 0 and 100 eV. All kinetic experiments were performed to at least 2.5 half-lives (81% reacted), and the relative rate constants are reproducible to  $\pm 15\%$ .

The iron sulfide ions were synthesized by reacting ethylene sulfide with  $\text{Fe}^+$ , reaction 1.<sup>11</sup> Each sulfide could be selectively generated either by



varying a continuous background pressure of the ethylene sulfide and controlling the reaction time or in a pulsed mode by controlling both the pulsed valve open time and the pressure of ethylene sulfide behind the pulsed valve.

## Results and Discussion

**Kinetics.**  $\text{Fe}^+$  through  $\text{FeS}_5^+$  were observed to follow excellent linear pseudo-first-order kinetics in reaction 1 for over 2.5 half-lives

(7) Carlin, T. J.; Freiser, B. S. *Anal. Chem.* **1983**, *55*, 571.

(8) Calculated using the Langevin equation with  $\alpha_{\text{Ar}} = 1.64 \text{ \AA}^3$ . From: Miller, T. M.; Bederson, B. *Adv. At. Mol. Phys.* **1977**, *13*, 49.

(9) Hettich, R. L.; Freiser, B. S. *ACS Symp. Ser.* **1987**, No. 359, Chapter 10.

(10) (a) Jacobson, D. B.; Freiser, B. S. *J. Am. Chem. Soc.* **1983**, *105*, 736.

(b) Jacobson, D. B.; Freiser, B. S. *J. Am. Chem. Soc.* **1983**, *105*, 7484.

(11) Carlin, T. J.; Wise, M. B.; Freiser, B. S. *Inorg. Chem.* **1981**, *20*, 2743.

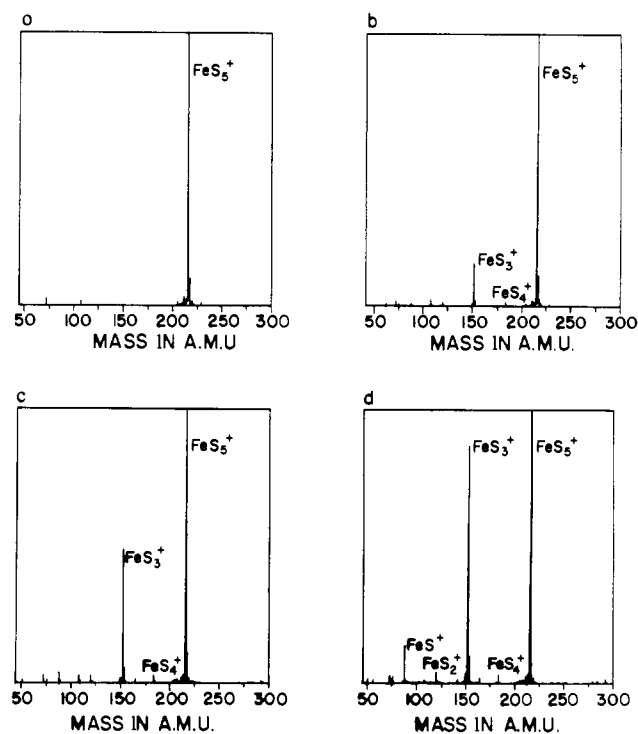


Figure 2. Photodissociation of  $\text{FeS}_5^+$  at (a) 0 s, (b) 2 s, (c) 6 s, and (d) 10 s with white light.

Table I. Relative Rate Constants for  $\text{FeS}_n^+$

reaction	rate, %	corrected rate, %
$\text{Fe}^+ + \text{SCH}_2\text{CH}_2$	100	100
$\text{FeS}^+ + \text{SCH}_2\text{CH}_2$	98	106
$\text{FeS}_2^+ + \text{SCH}_2\text{CH}_2$	94	110
$\text{FeS}_3^+ + \text{SCH}_2\text{CH}_2$	105	128
$\text{FeS}_4^+ + \text{SCH}_2\text{CH}_2$	51	64
$\text{FeS}_5^+ + \text{SCH}_2\text{CH}_2$	8	10

as exemplified in Figure 1 for  $\text{FeS}^+$ . These results suggest that in each case predominantly only one species was present, presumably a single isomeric ion in its ground state.  $\text{FeS}_6^+$  could not be examined in this manner, since it does not react with ethylene sulfide via simple sulfur abstraction. However, there is no evidence to indicate that  $\text{FeS}_6^+$  consists of more than one isomeric form, as discussed further below.

Table I lists the relative rate constants for  $\text{FeS}_n^+$  in reaction 1 obtained from the slopes of the kinetics plots and the background pressure of ethylene sulfide. The rate constant for  $\text{Fe}^+$  has been normalized to 100% in order to compare the rate constants for subsequent sulfur abstractions. Also given in Table I are the values corrected for the collision frequency of each ion which provide a direct comparison of the reaction efficiencies. Collision frequencies were obtained using the trajectory calculation of Su and Chesnovich<sup>12</sup> with  $\mu_{\text{D}}(\text{ethylene sulfide}) = 1.84 \text{ D}^{13}$  and  $\alpha(\text{ethylene sulfide}) = 6.73 \times 10^{-24} \text{ cm}^3$ .<sup>14</sup>

The general trend observed in Table I is that the first three sulfurs each add to  $\text{Fe}^+$  at approximately the same rate, followed by a dramatic drop in the efficiency to about half for  $\text{FeS}_4^+$ , one-tenth for  $\text{FeS}_5^+$ , and essentially zero for  $\text{FeS}_6^+$ . Possible explanations for why the reaction stops at  $\text{FeS}_6^+$  will be discussed.

**Photodissociation Spectra.** A typical example of the photodissociation observed for these species is shown in Figure 2 for

(12) Su, T.; Chesnovich, W. J. *J. Chem. Phys.* **1982**, *76*, 5183.

(13) *CRC Handbook of Chemistry and Physics*; Weast, R., Ed.; CRC Press: Boca Raton, FL, 1982.

(14) Calculated according to the method described in: Miller, K. J.; Savchik, J. A. *J. Am. Chem. Soc.* **1979**, *101*, 7206.

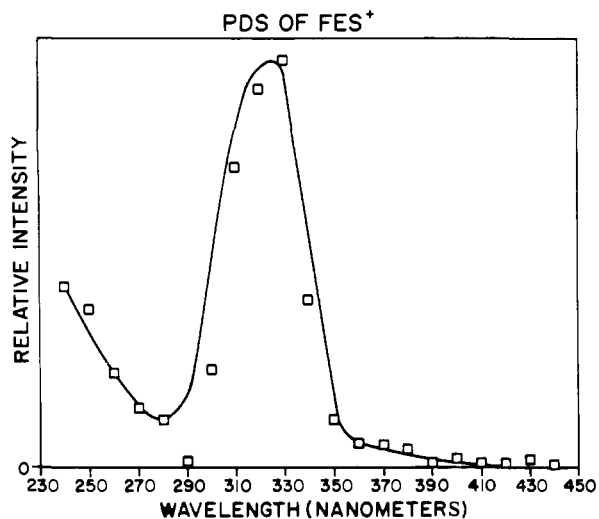


Figure 3. Photodissociation spectrum of  $FeS^+$ .

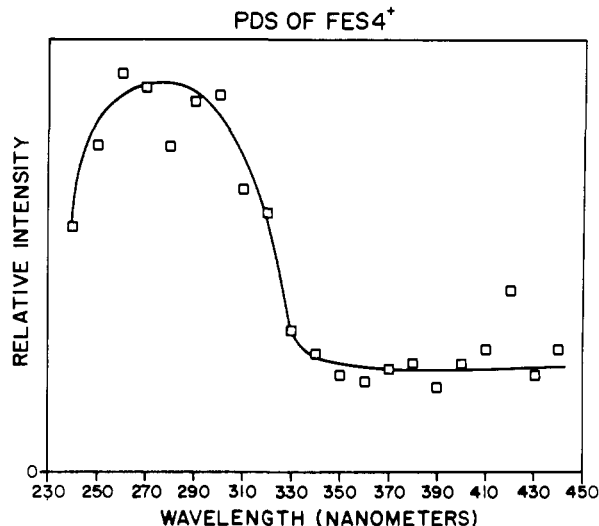


Figure 6. Photodissociation spectrum of  $FeS_4^+$ .

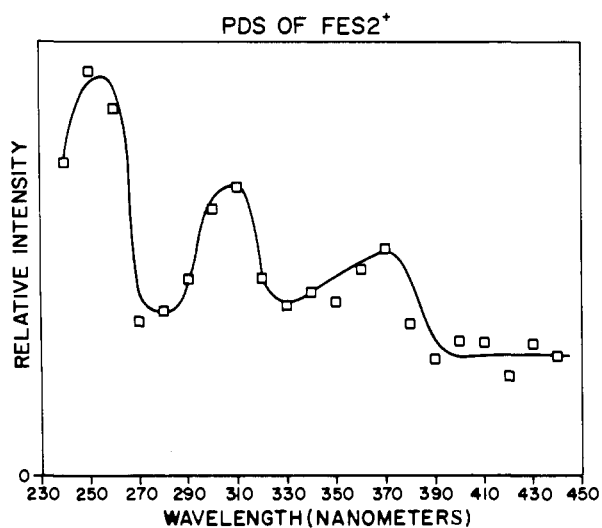


Figure 4. Photodissociation spectrum of  $FeS_2^+$ .

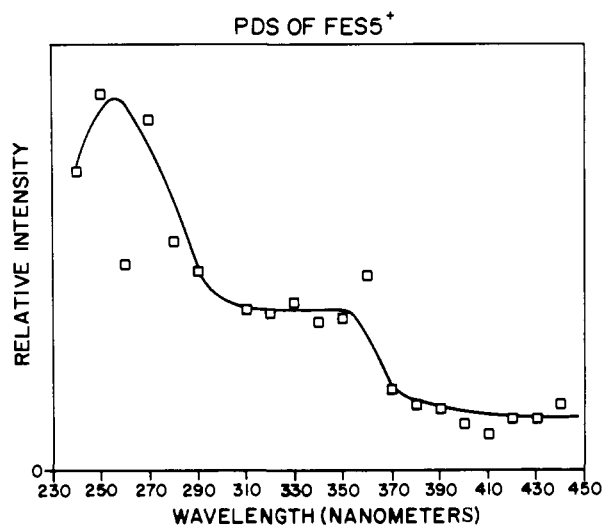


Figure 7. Photodissociation spectrum of  $FeS_5^+$ .

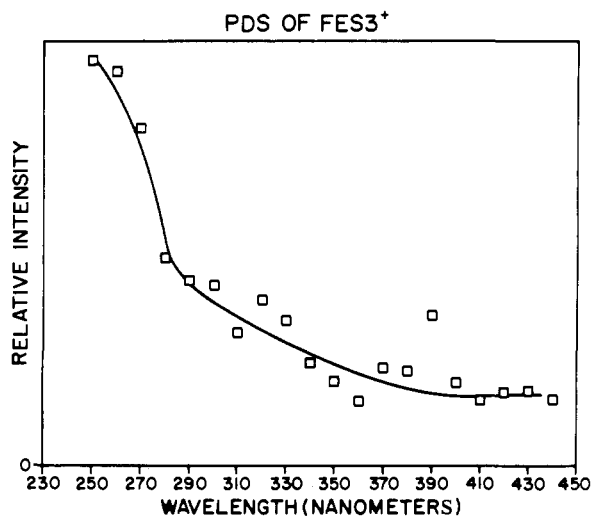


Figure 5. Photodissociation spectrum of  $FeS_3^+$ .

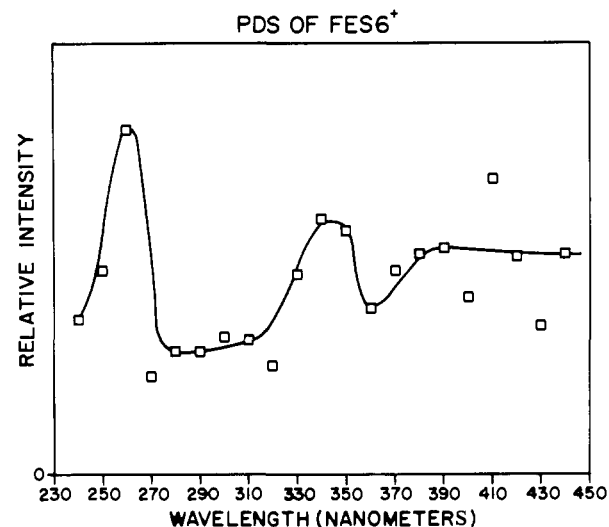


Figure 8. Photodissociation spectrum of  $FeS_6^+$ .

$FeS_5^+$  where, upon irradiation with white light, sequential  $S_2$  losses predominate over S loss.

The photodissociation spectra of  $FeS_n^+$  ( $n = 1-6$ ) are shown in Figures 3-8, respectively, with each spectrum the average of at least three separate spectra. The scatter in the individual spectra arising from low light levels and/or low cross sections made the existence of real band structure difficult to verify; the lines drawn

through the data, therefore, represent what are believed to be reasonable approximations of the actual spectra.

$FeS^+$  has a small absorption near 250 nm and an absorption from 290 to 350 nm with its maximum at 320 nm ( $\sigma = 0.3 \text{ \AA}^2$ ). These results can be compared to the spectrum of  $FeO^+$  which has two absorption bands centered at 260 and 350 nm with  $\sigma_{260}$

Table II. Thermodynamic Data for FeS<sup>+</sup>

parameter	value (kcal/mol)	further information
$D^{\circ}(\text{Fe}^+-\text{S})$	$61 \pm 6$	from PDS thresholds
$\text{IP}(\text{FeS})$	$200 \pm 8$ ( $8.7 \pm 0.4$ eV)	<i>a</i>
$\Delta H_f(\text{FeS}^+)$	$285 \pm 6$	<i>b</i>
$\Delta H_{\text{rxn},1}(n=0)$	$-2 \pm 6$	<i>b, c</i>

<sup>a</sup> Based on  $\Delta H_f(\text{FeS}) = 86 \pm 5$  kcal/mol from: Mills, K. C. *Thermodynamic Data for Inorganic Sulphides, Selenides and Tellurides*, 1974. <sup>b</sup> Based on  $\Delta H_f(\text{Fe}^+) = 280$  kcal/mol. <sup>c</sup> Based on  $\Delta H_f(\text{FeS}^+) = 285$  kcal/mol.

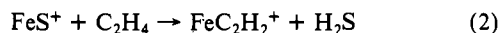
$= 0.07 \text{ \AA}^2$  and  $\sigma_{350} = 0.04 \text{ \AA}^2$ .<sup>15</sup> At this time it is unclear why FeS<sup>+</sup> has a much higher cross section than FeO<sup>+</sup>.

The photodissociation spectrum of FeS<sub>2</sub><sup>+</sup> is considerably different from the spectrum of FeS<sup>+</sup>. The major absorption peak in FeS<sub>2</sub><sup>+</sup> is shifted to shorter wavelength, around 260 nm ( $\sigma_{260} = 0.14 \text{ \AA}^2$ ), and has a broad absorption over the rest of the UV. The photodissociation spectrum of FeS<sub>3</sub><sup>+</sup> is similar to that of FeS<sub>2</sub><sup>+</sup> with a peak at around 240 nm ( $\sigma_{240} = 0.11 \text{ \AA}^2$ ) and a broad absorption to longer wavelengths. The photodissociation spectra of FeS<sub>4</sub><sup>+</sup>, FeS<sub>5</sub><sup>+</sup>, and FeS<sub>6</sub><sup>+</sup> all have absorption maxima near 260 nm with no other readily discernible peaks over the rest of the UV. The absolute cross sections for these ions are as follows: FeS<sub>4</sub><sup>+</sup>,  $\sigma_{280} = 0.30 \text{ \AA}^2$ ; FeS<sub>5</sub><sup>+</sup>,  $\sigma_{240} = 0.45 \text{ \AA}^2$ ; FeS<sub>6</sub><sup>+</sup>,  $\sigma_{250} = 0.68 \text{ \AA}^2$ .

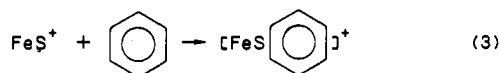
The photodissociation spectra of a number of other Fe<sup>+</sup>-L species also reveal absorption peaks near 250 nm. These species include L = C<sub>4</sub>H<sub>6</sub>, C<sub>6</sub>H<sub>6</sub>, CH<sub>3</sub>, O,<sup>15</sup> CH<sub>2</sub>,<sup>16</sup> OH, and CO.<sup>17</sup> Thus, we believe that the electronic transition that leads to this peak is likely to be metal localized and not a metal-ligand charge-transfer band. Beyond this, little information can be obtained from the spectra, and it is not clear why FeS<sup>+</sup> shows a much weaker absorption at 250 nm than any of the other iron sulfides. Further interpretation of these spectra must await detailed theoretical consideration.

### Thermochemistry

FeS<sup>+</sup>. Assuming that reaction 1 is exothermic yields  $D^{\circ}(\text{FeS}_n^+-\text{S}) > 59$  kcal/mol for  $n = 0-5$ . FeS<sup>+</sup> reacts with ethylene to lose H<sub>2</sub>S and form the iron-acetylene complex, reaction 2. The



absence of any displacement of S by ethylene, which suggests that  $D^{\circ}(\text{Fe}^+-\text{S}) > D^{\circ}(\text{Fe}^+-\text{C}_2\text{H}_4) = 34 \pm 2$  kcal/mol,<sup>18</sup> is in accord with the limit obtained from reaction 1. FeS<sup>+</sup> is observed to undergo only condensation with benzene, reaction 3. CID of the



condensation product yields exclusive loss of benzene, suggesting that  $D^{\circ}(\text{Fe}^+-\text{S}) > D^{\circ}(\text{Fe}^+-\text{benzene}) = 55 \pm 5$  kcal/mol.<sup>15</sup> The photodissociation threshold for the production of Fe<sup>+</sup> from FeS<sup>+</sup> has previously been reported from our laboratory at  $D^{\circ}(\text{Fe}^+-\text{S}) = 65 \pm 5$  kcal/mol.<sup>19</sup> This result is in good agreement with  $D^{\circ}(\text{Fe}^+-\text{S}) = 61 \pm 6$  kcal/mol obtained in this study, which in turn yields  $\Delta H_f(\text{FeS}^+) = 285 \pm 6$  kcal/mol.<sup>20</sup> From this heat of formation and assuming reaction 2 is exothermic, the limit  $D^{\circ}(\text{Fe}^+-\text{C}_2\text{H}_2) > 31 \pm 6$  kcal/mol is obtained. This result, together with the fact that ethylene readily displaces acetylene implying  $D^{\circ}(\text{Fe}^+-\text{C}_2\text{H}_2) < 34 \pm 2$  kcal/mol, yields an estimate for  $D^{\circ}(\text{Fe}^+-\text{C}_2\text{H}_2) = 32 \pm 6$  kcal/mol. The thermochemical

(15) Hettich, R. L.; Jackson, T. C.; Stanko, E. M.; Freiser, B. S. *J. Am. Chem. Soc.* **1986**, *108*, 5086.

(16) Hettich, R. L.; Freiser, B. S. *J. Am. Chem. Soc.* **1986**, *108*, 2537.

(17) Cassidy, C. J.; Freiser, B. S. *J. Am. Chem. Soc.* **1984**, *106*, 6176.

(18) Jacobson, D. B.; Freiser, B. S. *J. Am. Chem. Soc.* **1983**, *105*, 7492.

(19) Jackson, T. C.; Carlin, T. J.; Freiser, B. S. *Int. J. Mass Spectrom. Ion Processes* **1986**, *72*, 169.

(20) All heats of formation (and other supplementary values) are taken from: Lias, S. G.; Bartmess, J. E.; Liebman, J. F.; Holmes, J. L.; Levin, R. D.; Mallard, G. W. *J. Phys. Chem. Ref. Data, Suppl.* **1** **1988**, 17.

Table III. Thermodynamic Data for FeS<sub>2</sub><sup>+</sup>

parameter	value (kcal/mol)	further information
$D^{\circ}(\text{Fe}^+-\text{S}_2)$	$48 \pm 5$	from PDS thresholds
$D^{\circ}(\text{Fe}^+-2\text{S})$	$149 \pm 5$	<i>a, c</i>
$D^{\circ}(\text{FeS}^+-\text{S})$	$88 \pm 8$	<i>b, c</i>
$\Delta H_f(\text{FeS}_2^+)$	$263 \pm 5$	<i>a</i> and an S <sub>2</sub> unit lost
$\Delta H_{\text{rxn},1}(n=1)$	$-29 \pm 8$	<i>b, c</i>

<sup>a</sup> Based on  $\Delta H_f(\text{Fe}^+) = 280$  kcal/mol. <sup>b</sup> Based on  $\Delta H_f(\text{FeS}^+) = 285$  kcal/mol. <sup>c</sup> Based on  $\Delta H_f(\text{FeS}_2^+) = 263$  kcal/mol.

Table IV. Thermodynamic Data for FeS<sub>3</sub><sup>+</sup>

parameter	value (kcal/mol)	further information
$D^{\circ}(\text{FeS}_2^+-\text{S}_2)$	$49 \pm 5$	from PDS thresholds
$D^{\circ}(\text{Fe}^+-\text{S}_3)$	$47 \pm 8$	<i>a, d</i>
$D^{\circ}(\text{Fe}^+-3\text{S})$	$211 \pm 8$	<i>a, d</i>
$D^{\circ}(\text{FeS}_2^+-\text{S})$	$62 \pm 9$	<i>c, d</i>
$\Delta H_f(\text{FeS}_3^+)$	$267 \pm 8$	<i>b</i> and an S <sub>2</sub> unit lost
$\Delta H_{\text{rxn},1}(n=2)$	$-3 \pm 9$	<i>c, d</i>

<sup>a</sup> Based on  $\Delta H_f(\text{Fe}^+) = 280$  kcal/mol. <sup>b</sup> Based on  $\Delta H_f(\text{FeS}^+) = 285$  kcal/mol. <sup>c</sup> Based on  $\Delta H_f(\text{FeS}_2^+) = 263$  kcal/mol. <sup>d</sup> Based on  $\Delta H_f(\text{FeS}_3^+) = 267$  kcal/mol.

Table V. Thermodynamic Data for FeS<sub>4</sub><sup>+</sup>

parameter	value (kcal/mol)	further information
$D^{\circ}(\text{FeS}_2^+-\text{S}_2)$	$49 \pm 5$	from on PDS thresholds
$D^{\circ}(\text{Fe}^+-\text{S}_4)$	$70 \pm 7$	<i>a, e</i>
$D^{\circ}(\text{Fe}^+-2\text{S}_2)$	$96 \pm 7$	<i>a, e</i>
$D^{\circ}(\text{Fe}^+-4\text{S})$	$300 \pm 7$	<i>a, e</i>
$D^{\circ}(\text{FeS}^+-\text{S}_3)$	$74 \pm 9$	<i>b, e</i>
$D^{\circ}(\text{FeS}_3^+-\text{S})$	$88 \pm 11$	<i>d, e</i>
$\Delta H_f(\text{FeS}_4^+)$	$245 \pm 7$	<i>c</i> and an S <sub>2</sub> unit lost
$\Delta H_{\text{rxn},1}(n=3)$	$-29 \pm 11$	<i>d, e</i>

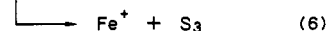
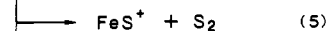
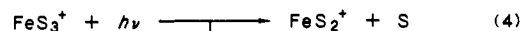
<sup>a</sup> Based on  $\Delta H_f(\text{Fe}^+) = 280$  kcal/mol. <sup>b</sup> Based on  $\Delta H_f(\text{FeS}^+) = 285$  kcal/mol. <sup>c</sup> Based on  $\Delta H_f(\text{FeS}_2^+) = 263$  kcal/mol. <sup>d</sup> Based on  $\Delta H_f(\text{FeS}_3^+) = 267$  kcal/mol. <sup>e</sup> Based on  $\Delta H_f(\text{FeS}_4^+) = 245$  kcal/mol.

information obtained for FeS<sup>+</sup> is listed in Table II.

FeS<sub>n</sub><sup>+</sup> ( $n = 2-6$ ). FeS<sub>2</sub><sup>+</sup> is unreactive with ethylene but does react with benzene by displacement of S<sub>2</sub> exclusively, suggesting that  $34 \pm 2$  kcal/mol  $< D^{\circ}(\text{Fe}^+-\text{S}_2) \leq 55 \pm 5$  kcal/mol. Photodissociation of FeS<sub>2</sub><sup>+</sup> results mainly in loss of S<sub>2</sub> with very little loss of S. The threshold near 600 nm gives a bond energy of  $D^{\circ}(\text{Fe}^+-\text{S}_2) = 48 \pm 5$  kcal/mol, well within the limits suggested above.

Using  $D^{\circ}(\text{Fe}^+-\text{S}_2) = 48$  kcal/mol determined above yields  $\Delta H_f(\text{FeS}_2^+) = 263 \pm 5$  kcal/mol, which can then be used to calculate several other thermochemical values, Table III. The most interesting value to examine is  $D^{\circ}(\text{FeS}^+-\text{S}) = 88 \pm 8$  kcal/mol, which can be compared to  $D^{\circ}(\text{Fe}^+-\text{S}) = 61 \pm 6$  kcal/mol, indicating an apparently large synergistic effect.

Photodissociation of FeS<sub>3</sub><sup>+</sup> results in three products, reactions 4-6, with reaction 5, the loss of S<sub>2</sub>, by far the most dominant



process. The photodissociation threshold for reaction 5 at approximately 584 nm gives  $D^{\circ}(\text{FeS}^+-\text{S}_2) = 49 \pm 5$  kcal/mol, from which  $\Delta H_f(\text{FeS}_3^+) = 267 \pm 8$  kcal/mol is calculated. A number of other thermochemical values can also be calculated and these are found in Table IV.

Photodissociation of both FeS<sub>4</sub><sup>+</sup> and FeS<sub>5</sub><sup>+</sup> once again yields loss of S<sub>2</sub> as the predominant product at all of the wavelengths monitored. The photodissociation thresholds yield the values  $D^{\circ}(\text{FeS}_2^+-\text{S}_2) = 49 \pm 5$  kcal/mol and  $D^{\circ}(\text{FeS}_3^+-\text{S}_2) = 43 \pm 5$  kcal/mol from which  $\Delta H_f(\text{FeS}_4^+) = 245 \pm 7$  kcal/mol and  $\Delta H_f(\text{FeS}_5^+) = 255 \pm 9$  kcal/mol are calculated, respectively.

Table VI. Thermodynamic Data for  $\text{FeS}_3^+$ 

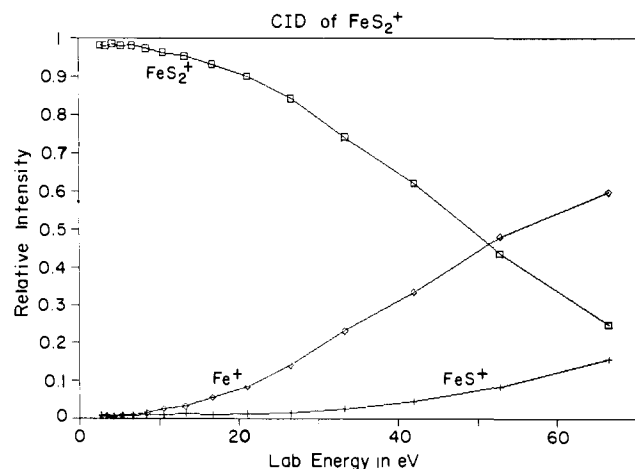
parameter	value (kcal/mol)	further information
$D^\circ(\text{FeS}_3^+-\text{S}_2)$	$43 \pm 5$	from PDS thresholds
$D^\circ(\text{Fe}^+-\text{S}_3)$	$51 \pm 9$	a, f
$D^\circ(\text{Fe}^+-\text{S}_3\text{S}_2)$	$90 \pm 9$	a, f
$D^\circ(\text{Fe}^+-\text{S}_4\text{S})$	$126 \pm 9$	a, f
$D^\circ(\text{Fe}^+-5\text{S})$	$356 \pm 9$	a, f
$D^\circ(\text{FeS}^+-\text{S}_4)$	$65 \pm 11$	b, f
$D^\circ(\text{FeS}^+-2\text{S}_2)$	$91 \pm 11$	b, f
$D^\circ(\text{FeS}_2^+-\text{S}_3)$	$42 \pm 10$	c, f
$D^\circ(\text{FeS}_2^+-\text{S})$	$56 \pm 11$	e, f
$\Delta H_f(\text{FeS}_3^+)$	$255 \pm 9$	d and an $\text{S}_2$ unit lost
$\Delta H_{\text{rxn.1}}(n=4)$	$3 \pm 11$	e, f

<sup>a</sup> Based on  $\Delta H_f(\text{Fe}^+) = 280$  kcal/mol. <sup>b</sup> Based on  $\Delta H_f(\text{FeS}^+) = 285$  kcal/mol. <sup>c</sup> Based on  $\Delta H_f(\text{FeS}_2^+) = 263$  kcal/mol. <sup>d</sup> Based on  $\Delta H_f(\text{FeS}_3^+) = 267$  kcal/mol. <sup>e</sup> Based on  $\Delta H_f(\text{FeS}_4^+) = 245$  kcal/mol. <sup>f</sup> Based on  $\Delta H_f(\text{FeS}_5^+) = 255$  kcal/mol.

Table VII. Thermodynamic Data for  $\text{FeS}_6^+$ 

parameter	value (kcal/mol)	further information
$D^\circ(\text{FeS}_4^+-\text{S}_2)$	$38 \pm 5$	PDS threshold and displacement with ethylene
$D^\circ(\text{Fe}^+-\text{S}_6)$	$66 \pm 9$	a, g
$D^\circ(\text{Fe}^+-3\text{S}_2)$	$134 \pm 9$	a, g
$D^\circ(\text{Fe}^+-2\text{S}_3)$	$110 \pm 9$	a, g
$D^\circ(\text{Fe}^+-\text{S}_4\text{S}_2)$	$108 \pm 9$	a, g
$D^\circ(\text{Fe}^+-6\text{S})$	$439 \pm 9$	a, g
$D^\circ(\text{FeS}^+-\text{S}_5)$	$73 \pm 11$	b, g
$D^\circ(\text{FeS}_2^+-\text{S}_4)$	$60 \pm 10$	c, g
$D^\circ(\text{FeS}_2^+-2\text{S}_2)$	$86 \pm 10$	c, g
$D^\circ(\text{FeS}_3^+-\text{S}_3)$	$63 \pm 12$	d, g
$D^\circ(\text{FeS}_3^+-\text{S})$	$83 \pm 13$	f, g
$\Delta H_f(\text{FeS}_6^+)$	$238 \pm 9$	d and an $\text{S}_2$ lost
$\Delta H_{\text{rxn.1}}(n=5)$	$-24 \pm 13$	f, g

<sup>a</sup> Based on  $\Delta H_f(\text{Fe}^+) = 280$  kcal/mol. <sup>b</sup> Based on  $\Delta H_f(\text{FeS}^+) = 285$  kcal/mol. <sup>c</sup> Based on  $\Delta H_f(\text{FeS}_2^+) = 263$  kcal/mol. <sup>d</sup> Based on  $\Delta H_f(\text{FeS}_3^+) = 267$  kcal/mol. <sup>e</sup> Based on  $\Delta H_f(\text{FeS}_4^+) = 245$  kcal/mol. <sup>f</sup> Based on  $\Delta H_f(\text{FeS}_5^+) = 255$  kcal/mol. <sup>g</sup> Based on  $\Delta H_f(\text{FeS}_6^+) = 238$  kcal/mol.

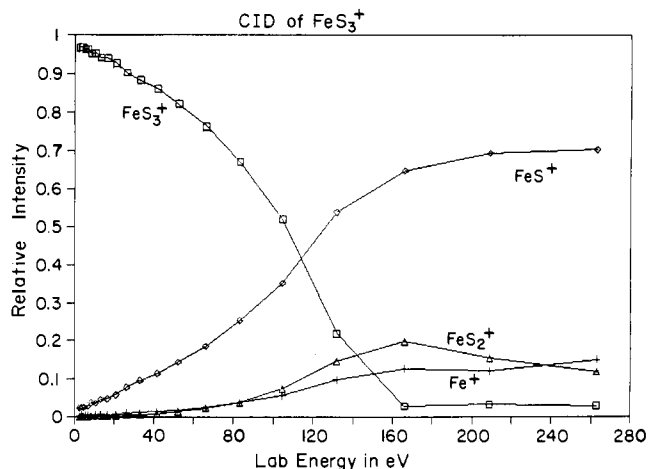
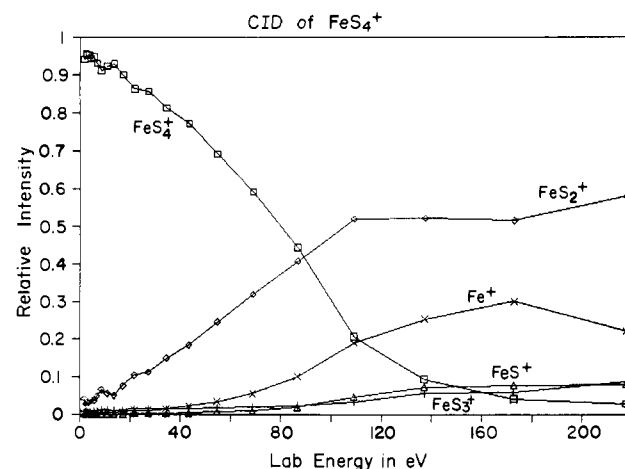
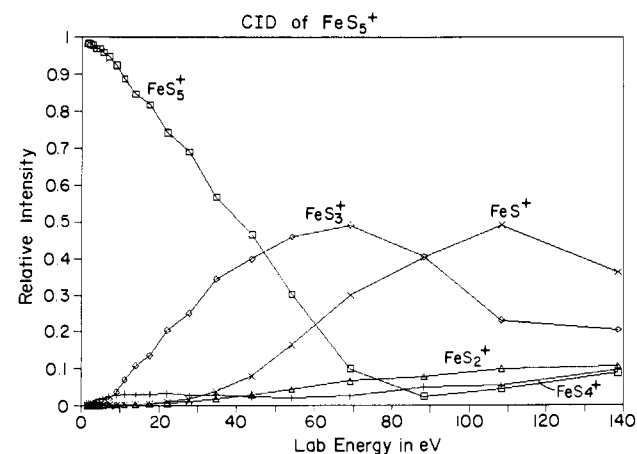
Figure 9. CID breakdown curve for  $\text{FeS}_2^+$ .

Tables V and VI list the various thermochemical values for these systems.

A threshold for the loss of  $\text{S}_2$  from  $\text{FeS}_6^+$  was not seen with our lowest filter value of 43 kcal/mol, but when  $\text{FeS}_6^+$  was reacted with ethylene no displacement was observed. From these two observations a bond energy of  $D^\circ(\text{FeS}_4^+-\text{S}_2) = 38 \pm 5$  kcal/mol is assigned yielding  $\Delta H_f(\text{FeS}_6^+) = 238 \pm 9$  kcal/mol. Other related thermochemical values are given in Table VII.

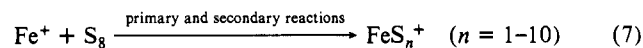
#### Collision-Induced Dissociation (CID) Studies

CID breakdown curves for  $\text{FeS}_n^+$  ( $n = 2-6$ ) generated from reaction 1 are shown in Figures 9-13. In accordance with the

Figure 10. CID breakdown curve for  $\text{FeS}_3^+$ .Figure 11. CID breakdown curve for  $\text{FeS}_4^+$ .Figure 12. CID breakdown curve for  $\text{FeS}_5^+$ .

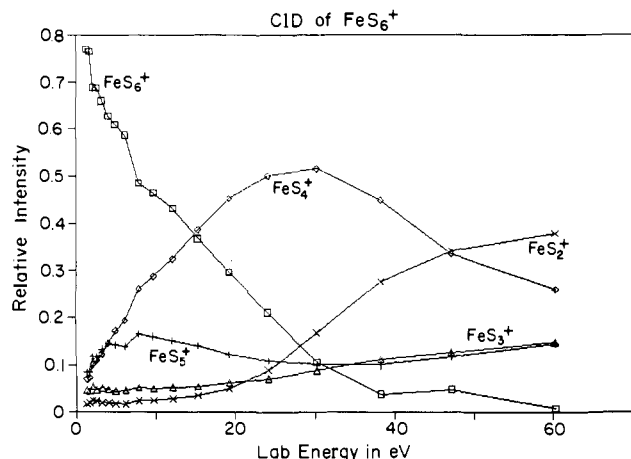
photodissociation results, CID yields primarily loss of multiple  $\text{S}_2$  units with the loss of an odd number of sulfurs growing at higher energies, but never predominating.

In a parallel study,<sup>21</sup>  $\text{Fe}^+$  has been observed to react with elemental sulfur,  $\text{S}_8$ , in the gas phase to generate  $\text{FeS}_n^+$  ( $n = 1-10$ ), reaction 7. Interestingly, each of these species was also observed



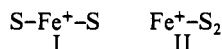
to undergo collision-induced dissociation predominantly by sequential loss of  $\text{S}_2$  molecules.

(21) Gord, J. R.; Bemish, R.; Freiser, B. S., unpublished results.

Figure 13. CID breakdown curve for  $\text{FeS}_6^+$ .

### Implications for Ion Structures

**$\text{FeS}_2^+$  and  $\text{FeS}_3^+$ .** There are two possible structures for  $\text{FeS}_2^+$ , iron bound to two distinct sulfur atoms, structure I, or iron bound to an  $\text{S}_2$  molecule, structure II. Photodissociation, CID and the

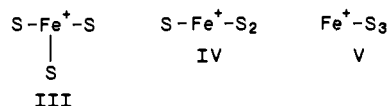


displacement reaction with benzene all suggest structure II in which the sulfurs are coupled together. Photodissociation and CID of structure I would be expected to show loss of  $\text{S}_2$  at low photon and collision energies, where a longer ion lifetime would facilitate rearrangement, but at higher energies a larger percentage of direct cleavage of S atom would be expected. However, loss of atomic sulfur was not observed to predominate at the higher energies.

The thermochemistry described above for  $\text{FeS}_2^+$  also adds support for structure II. Of particular significance is the comparison between  $D^\circ(\text{FeS}^+-\text{S}) = 88 \pm 8$  kcal/mol and  $D^\circ(\text{Fe}^+-\text{S}) = 61 \pm 6$  kcal/mol. One might expect both sulfurs to be bound with approximately the same bond strength, or with the second sulfur perhaps being bound a little more or less tightly than the first. A difference of about 27 kcal/mol, therefore, indicates that the sulfurs are probably not separately bound to  $\text{Fe}^+$  as in structure I, but exist as an  $\text{S}_2$  structure II. Figure 14 summarizes the results in a thermochemical cycle for the  $\text{FeS}_2^+$  species.

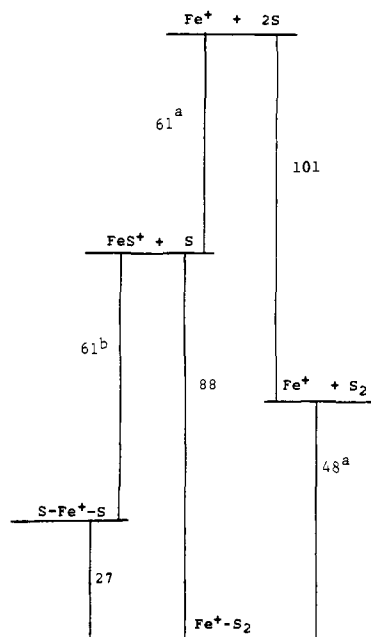
Interestingly, there are several precedents for structure II in nature including Pyrite<sup>22</sup> which also consists of an iron bound to a discrete  $\text{S}_2$  molecule. Finally, the few examples of these types of structures in the literature show the  $\text{S}_2$  molecule to be  $\pi$  bound and not  $\sigma$  bound.<sup>23</sup> Unfortunately, our experimental results do not provide such detailed structural information.

Structures III through V are possible for the  $\text{FeS}_3^+$  species.



Structure III is the least likely and can be ruled out for several reasons. First, in analogy to the disulfide case, three separately bonded sulfurs would likely result in a higher energy species. Secondly, if the structure was a trisulfide,  $\text{S}_2$  and  $\text{S}_3$  loss would be expected at low CID energies, but at higher energies loss of S by direct cleavage should predominate and this is not observed. Finally, assuming a formal oxidation state of  $\text{S}^{2-}$  and  $\text{S}_n^{2-}$  ( $n \geq 2$ ), the iron in structure III would be in a less favorable +7 oxidation state.

Structure IV, however, is compelling on the basis of the observed fragmentation and thermochemistry. The difference in bond



a) From photodissociation thresholds.  
b) Based on the assumption that  $D^\circ(\text{FeS}^+-\text{S}) = D^\circ(\text{Fe}^+-\text{S})$

Figure 14. Thermochemical cycle for  $\text{FeS}_2^+$ .

energies between  $D^\circ(\text{FeS}^+-\text{S}_2) = 49$  kcal/mol and  $D^\circ(\text{Fe}^+-\text{S}_3) = 47$  kcal/mol is insignificant. Thus, for structure V with iron bound to  $\text{S}_3$ , loss of  $\text{S}_3$  would be expected to predominate in the photodissociation and CID spectra, particularly at higher energies. This, however, is not the case. It is also interesting to compare  $D^\circ(\text{FeS}_2^+-\text{S}) = 62$  kcal/mol to  $D^\circ(\text{Fe}^+-\text{S}) = 61$  kcal/mol and  $D^\circ(\text{FeS}^+-\text{S}_2) = 49$  kcal/mol to  $D^\circ(\text{Fe}^+-\text{S}_2) = 48$  kcal/mol which, although not conclusive, is certainly suggestive of structure IV.

**$\text{FeS}_n^+$  ( $n = 4-6$ ).** As the number of sulfurs increases, the variety of possible structures also increases. Of these structures, the predominant loss of multiple  $\text{S}_2$  units in both the CID and photodissociation spectra suggest as likely structures  $\text{Fe}(\text{S}_2)_2^+$ ,  $\text{Fe}(\text{S}_2)_3^+$ , and  $\text{Fe}(\text{S}_2)_n^+$  for  $\text{FeS}_n^+$ ,  $n = 4-6$ , respectively. Complicating this picture, however, is the observation that  $\text{FeS}_n^+$ ,  $n = 7-10$ , generated from elemental sulfur by reaction 7, also undergoes CID predominantly by multiple  $\text{S}_2$  loss, as mentioned above. For these species, the structures  $\text{Fe}(\text{S}_2)_{n+1}^+$  and  $\text{Fe}(\text{S}_2)_n\text{S}^+$ ,  $n = 3$  and 4, are not possible since they result in unreasonable oxidation states of iron (i.e., +9 and +11, respectively). Thus, it is apparent that  $\text{S}_2$  loss during CID or photodissociation may not be very diagnostic of the structure.

Ring structures are common in metal sulfide compounds<sup>2,3</sup> and undoubtedly are involved in the polysulfide species  $\text{FeS}_n^+$ ,  $n = 7-10$ . Any combination of rings,  $\text{S}_2$  units, and S atoms bound to iron is possible provided the oxidation state of iron does not exceed +7. In analogy to the reported structure of  $\text{MoS}_9^{2-}$ ,<sup>3</sup> for example,  $\text{FeS}_9$  could consist of two  $\text{S}_4$  rings and an atomic sulfur bound to iron. Also of particular relevance is the observation that metal polysulfide ring structures in solution frequently dissociate by losing  $\text{S}_2$ . Thus, the presence of such ring structures cannot be conclusively ruled out for  $\text{FeS}_n^+$  ( $n = 4-6$ ).

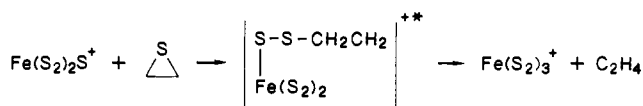
Structures involving only individual sulfurs bound to the metal center are not possible for  $\text{FeS}_n^+$  ( $n > 3$ ), once again because they would result in unreasonable oxidation states of iron. The thermochemical data in Tables IV-VII indicate that loss of  $\text{S}_3$  from  $\text{FeS}_3^+$  and  $\text{FeS}_5^+$  is the only other process lower in energy than loss of  $\text{S}_2$ . However, as discussed above for  $\text{FeS}_3^+$ , the fact that loss of  $\text{S}_3$  never predominates in the CID and photodissociation spectra of these two ions tends to make structures involving  $\text{S}_3$  less likely.

In summary, these arguments suggest that structures involving either coordinated  $\text{S}_2$  units or small polysulfide rings describe the  $\text{FeS}_n^+$ ,  $n = 4-6$ , species. Although CID and photodissociation

(22) Cotton, A. F.; Wilkinson, G. *Advanced Inorganic Chemistry*, 4th ed.; Wiley: New York, 1980.

(23) (a) Dines, M. *Inorg. Chem.* 1978, 17, 762. (b) Ziegler, T. *Inorg. Chem.* 1986, 25, 2721.

## Scheme I



result in multiple  $\text{S}_2$  losses, such losses are possible from either type of structure. In addition, the thermochemistry obtained in Tables IV-VII for these species do not distinguish between these two types of structure.

It is interesting to try to rationalize the observed reactivity of these species with ethylene sulfide, summarized in Table I, in terms of the possible structures. Oxidative addition of ethylene sulfide to the metal center should only be facile provided that the intermediate species not exceed the +7 oxidation state of iron. Assuming the structures  $\text{Fe}(\text{S}_2)_n^+$  and  $\text{Fe}(\text{S}_2)_{n-1}\text{S}^+$  for  $n = 1-3$ , this would predict a sharp reduction in reactivity for  $\text{Fe}(\text{S}_2)_2\text{S}^+$  and  $\text{Fe}(\text{S}_2)_3^+$  where oxidative addition to the ethylene sulfide would proceed through a +9 intermediate. This, in fact, is what is observed for reaction 1 in Table I. In contrast, the  $\text{Fe}(\text{S})$  ( $\text{S}_4$ )<sup>+</sup> and  $\text{Fe}(\text{S}_2)$  ( $\text{S}_4$ )<sup>+</sup>, representative of possible ring structures for  $\text{FeS}_5^+$  and  $\text{FeS}_6^+$ , respectively, could react with ethylene sulfide by oxidative addition proceeding through an "allowed" +7 oxidation state of iron. Finally, the observed reactivity of  $\text{FeS}_5^+$ , although substantially reduced, suggests either the presence of a ring structure or that a mechanism not involving oxidative

addition can occur as postulated in Scheme I.

## Conclusion

Photodissociation, CID, and kinetic methods were used to study various iron sulfides generated from sequential reactions with ethylene sulfide. The kinetic behavior of the sulfides indicates a homogeneous population in each case and, thus, they are believed to be predominantly thermalized and consisting mainly of one isomer. The last two sulfur abstractions were found to be substantially slower than the first four.

CID and photodissociation studies showed predominant loss of  $\text{S}_2$  with little or no loss of S atom. While these results are consistent with structures involving coordinated  $\text{S}_2$  units, polysulfide ring structures also dissociate by  $\text{S}_2$  loss and cannot be ruled out for  $\text{FeS}_n^+$ ,  $n = 4-6$ . Photodissociation thresholds provided absolute bond energies for the iron sulfides, from which various thermochemical values were calculated. These data yield loss of either  $\text{S}_2$  or  $\text{S}_3$  as the lowest energy process for these species.

**Acknowledgement** is made to the Division of Chemical Sciences in the Office of Basic Energy Sciences in the U.S. Department of Energy (DE-FG02-87ER13766) for supporting this research and to the National Science Foundation (CHE-8612234) for providing funds for the advancement of FTMS methodology. The authors also thank Ian Rothwell for helpful discussions.

**Registry No.**  $\text{Fe}^+$ , 14067-02-8;  $\text{FeS}^+$ , 60173-22-0; ethylene sulfide, 420-12-2.

## Time-Resolved Studies of "Salt Effects" on Weak Acid Dissociation

J. Lee

Contribution from the Picosecond and Quantum Radiation Laboratory, P.O. Box 4260, Texas Tech University, Lubbock, Texas 79409. Received February 8, 1988

**Abstract:** Using the photon initiated weak acid 2-naphthol as a probe for local structure on subnanosecond time scales, a variety of specific effects, including quenching of the excited state, and various degrees of enhancement or inhibition of the proton dissociation process have been observed. Both urea and  $\text{Na}_2\text{SO}_4$  up to molar concentrations are inert toward the proton dissociation reaction. The most common behavior is exhibited by  $\text{LiCl}$ ,  $\text{NaCl}$ ,  $\text{KCl}$ ,  $\text{MgCl}_2$ , and  $\text{CaCl}_2$ . At different "critical" concentrations, specific for each salt, they totally block the otherwise fast proton dissociation process. The latter result is believed to be caused by hydration of cations and anions and the consequent loss of "free" water molecules necessary for the rapid production of  $(\text{H}_3\text{O}_4)^+$ . At lower concentrations there is active competition between the hydrated ions and the proton for available "free" water. A "kinetic solvation number" for each electrolyte system, determined from a random walk matrix analysis, is used to explain the observed results. These experiments are the first that are capable of investigating the "chemical structure" of outer-sphere hydration shells of simple ions.

Picosecond and femtosecond kinetic spectroscopies are changing the way chemical reactions are regarded. Continuum models<sup>1-3</sup> are having to be replaced by molecular-level descriptions. Weak acid processes in aqueous media containing ions or polar solutes is yet another example where these new methods can make an impact. Such processes form a part of a wider class of ionic reactions in aqueous salt solutions that play a major role in chemistry. Understanding chemical reactions in ionic solutions is also important in biology<sup>4</sup> where primary processes such as

charge transfer take place in an ionic environment.

Because of the strongly different acidities<sup>5-9</sup> of 2-naphthol in its ground (2-ROH,  $\text{p}K_a = 9.8$ ) and electronically excited (2-ROH\*,  $\text{p}K_a^* = 2.6$ ) states, this molecule can be utilized as a "photon initiated acid".<sup>8,9</sup> When the acid state is formed by an ultrashort light pulse, associated changes in the surrounding liquid medium can be probed on the nanosecond time scale of the 2-ROH\* lifetime. Because of this brief lifetime, only the most rapid deprotonation reactions are detected by this technique. For example, it was found<sup>8,9</sup> that proton dissociation from 2-ROH\* is immeasurably slow in pure alcohol but can be activated by a water "cluster" having a minimum of four molecules. The proton dis-

(1) (a) Harned, H. S.; Owen, B. B. *The Physical Chemistry of Electrolytic Solutions*, 3rd ed.; Reinhold: New York, 1958. (b) Robinson, R. A.; Stokes, R. H. *Electrolyte Solutions*, 2nd revised ed.; Butterworths: London, 1965. (c) Bockris, J. O'M.; Reddy, A. K. N. *Modern Electrochemistry*; Plenum: New York, 1970.

(2) Hasted, J. B. *Aqueous Dielectrics*; Chapman and Hall: London, 1973.

(3) Smedley, S. I. *The Interpretation of Ionic Conductivity in Liquids*; Plenum: New York, 1980.

(4) *Water and Ions in Biological Systems*; Pullman, A., Vasilescu, V., Packer, L., Eds.; Plenum: New York, 1985.

(5) Forster, Th. *Z. Electrochem.* **1950**, *54*, 531.

(6) Weller, A. *Z. Electrochem.* **1952**, *56*, 662.

(7) Weller, A. *Z. Physik. Chem. (Frankfurt am Main)* **1958**, *17*, 224.

(8) Lee, J.; Griffin, R. D.; Robinson, G. W. *J. Chem. Phys.* **1985**, *82*, 4920.

(9) Lee, J.; Robinson, G. W.; Webb, S. P.; Phillips, L. A.; Clark, J. H. *J. Am. Chem. Soc.* **1986**, *108*, 6538.